ScienceDirect

ELSEVIER

Analytica Chimica Acta 588 (2007) 283–291

ANALYTICA CHIMICA ACTA

www.elsevier.com/locate/aca

Electrochemical oxidation of ochratoxin A at a glassy carbon electrode and *in situ* evaluation of the interaction with deoxyribonucleic acid using an electrochemical deoxyribonucleic acid-biosensor

S.C.B. Oliveira [a], V.C. Diculescu [a], G. Palleschi [b], D. Compagnone [c], A.M. Oliveira-Brett [a,*]

[a] *Departamento de Química, Faculdade de Ciências e Tecnologia, Universidade de Coimbra, 3004-535 Coimbra, Portugal*
[b] *Dipartimento di Scienze e Tecnologie Chimiche, Università Tor Vergata, via della Ricerca Scientifica, 00133 Rome, Italy*
[c] *Dipartimento di Scienze degli Alimenti, Università di Teramo, via Lerici 1, Mosciano S. Angelo, 64023 Teramo, Italy*

Received 16 November 2006; received in revised form 6 February 2007; accepted 13 February 2007
Available online 20 February 2007

Abstract

Ochratoxin A (OTA) is a fungal metabolite that occurs in foods, beverages, animal tissues, human blood and presents carcinogenic, teratogenic and nephrotoxic properties. This study concerns the redox properties of OTA using electrochemical techniques which have the potential for providing insights into the biological redox reactions of this molecule. The *in situ* evaluation of the OTA interaction with DNA using a DNA-electrochemical biosensor is also reported.

The oxidation of OTA is an irreversible process proceeds with the transfer of one electron and one proton in a diffusion-controlled mechanism. The diffusion coefficient of OTA was calculated in pH 7 phosphate buffer to be $D_O = 3.65 \times 10^{-6}$ cm^2 s^{-1}. The oxidation of OTA is also pH dependent for electrolytes with pH < 7 and involves the formation of a main oxidation product which adsorbs strongly at the GCE surface undergoing reversible oxidation. In alkaline electrolytes OTA undergoes chemical deprotonation, the oxidation involving only the transfer of one electron.

The electrochemical dsDNA-biosensor was also used to evaluate the possible interaction between OTA and DNA. The experiments have clearly proven that OTA interacts and binds to dsDNA strands immobilized onto a GCE surface, but no evidence of DNA-damage caused by OTA was obtained.

Keywords: Ochratoxin A; Deoxyribonucleic acid; Oxidative damage; Oxidation; Voltammetry; Electroanalytical determination; Interferences

1. Introduction

Mycotoxins [1] are a structurally diverse group of compounds produced by the secondary metabolism of fungi. Among mycotoxins, ochratoxins represent the group of metabolites produced by *Aspergillus ochraceus* and, more commonly, by *Penicillium viricatum*. The ochratoxins comprise a polyketide-derived dihydroisocoumarin moiety linked via its 12-carboxyl group to L-β-phenylalanine by an amide bond [2–4].

Several ochratoxins are described in the literature, but the most important one appears to be ochratoxin A (OTA), Scheme 1, a substance that frequently occurs in improperly stored food (cereals, coffee, milk) and beverages (beer and wine) [5,6]. Upon adsorption from the gastrointestinal tract, OTA can easily reach the bloodstream and be bound to the serum proteins. Readsorption of OTA from the intestine back to the circulation, as a consequence of biliary recycling, favours the systemic redistribution of OTA towards different tissues. The kidneys are the organs most susceptible to OTA since it was shown that accumulation can cause both acute and chronic lesions by induction of a defect in the anion transport mechanism. In addition, immunotoxic, teratogenic and carcinogenic effects of OTA are described in animals, mainly in rats and mice [6].

In terms of OTA genotoxicity, the toxin promotes oxidative stress [7,8], oxidative base damage [8] and single strand DNA cleavage through production of reactive oxygen species (ROS) [9,10]. However, the mechanism of OTA-induced tumour for-

* Corresponding author. Tel.: +351 239 835295; fax: +351 239 835295.
E-mail address: brett@ci.uc.pt (A.M. Oliveira-Brett).

0003-2670/$ – see front matter © 2007 Elsevier B.V. All rights reserved.
doi:10.1016/j.aca.2007.02.029

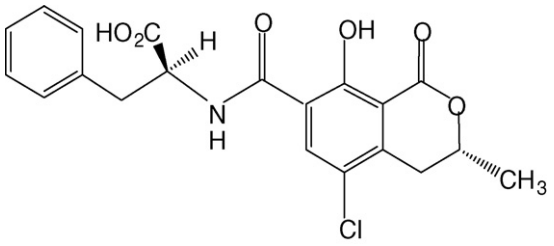

Scheme 1. Chemical structure of ochratoxin A.

mation is unknown and conflicting results have been reported regarding the potential of OTA to bind to DNA. For example, it was shown that *in vivo* OTA is poorly metabolized and no reactive intermediates capable of interacting with DNA have been detected [11]. Contrary to this, *in vitro*, a hydroquinone/quinone redox couple and a carbon-bonded OTA-deoxyguanosine adduct formed by electrochemical oxidation and photoreaction of OTA have been reported and suggested to be involved in OTA carcinogenicity [12]. Also, it has been stated that the redox-active transition metals may play an important role in OTA activation. The results reported demonstrated that OTA can facilitate oxidative DNA strand scission in the presence of copper without the aid of an external reducing agent [13]. Moreover, the protective effect of some substances able to act as ROS scavengers has been investigated through various biological assays, with an overall protective effect of vitamins A, C, and E [14] as well as of anthocyanins [15].

As a result of the importance of OTA in biological systems, there is an increasing need for developing methods for the detection and determination of mycotoxins in food, beverages and biological fluids [16]. Although the most used technique for the detection of OTA is HPLC with fluorescence detection due to the fact that OTA possesses natural fluorescence [17], other analytical methods such as capillary electrophoresis [18], radioimmunoassay [19] and enzyme-linked immunosorbent assay [20,21] have been developed. However, more recently, there has been a tendency for the use of less costly techniques and a reduction in the use of organic solvents since they result in high ecological costs.

Due to their high sensitivity, voltammetric methods have been successfully used for the detection and determination of various biological compounds. Moreover, investigations of the redox behaviour of biologically occurring compounds by means of electrochemical techniques have the potential for providing valuable insights into the redox reactions of these molecules [22,23].

Concerning OTA, investigation on its oxidation behaviour has been carried out at a glassy carbon electrode (GCE), but only in specific conditions using organic solvents or aqueous media with pH between 6 and 8 and using cyclic voltammetry [24]. Those results were compared with the oxidation behaviour of 4-chlorophenol. It was shown that the electrochemical oxidation of OTA in acetonitrile solutions corresponds to the removal of protons and electrons from the phenolic moiety to form a cationic intermediate with subsequent formation of a quinone species. In aqueous buffer, a single irreversible peak was found, the oxidative process yielding only a phenoxyl radical. No oxidation product of OTA electrochemically detected was observed, and more work should be done to fully characterize the OTA electrochemical redox mechanism.

On the other hand, in the context of OTA-produced DNA damage, oxidation of OTA was also studied in the presence of transition metal ions [13] and of a Fe-porphyrin system that led to a model for the enzymatic activation of OTA and DNA cleavage [12]. Upon oxidation of OTA with the Fe-porphyrin/H_2O_2 system and subsequent reduction by ascorbate, a hydroquinone specie was detected by HPLC. This led to the conclusion that a quinone derivative of OTA may play an important role in OTA-mediated genotoxicity. However, in spite of these results, the genotoxic effects of OTA are still questioned [19,25], especially *in vivo*, where DNA adducts and DNA damage could occur from secondary effects.

In the past decade, there has been great interest in the development of DNA based biosensors. An electrochemical sensor for DNA damage consists of an electrode with DNA immobilized on the surface. Interactions of surface-immobilized DNA (either by electrostatic adsorption or by evaporation) with the damaging agent are converted, via changes in electrochemical properties of the DNA recognition layer, into measurable electrical signals. Such a kind of device has been successfully applied to study the interaction of several substances with dsDNA and the interpretation of the results contributed to the elucidation of the mechanisms by which DNA is damaged by hazardous compounds [26].

In this context, the present study is concerned with the electrochemical characterization of OTA oxidation behaviour, for a wide pH range between 2 and 12, using cyclic, square wave and differential pulse voltammetry at a glassy carbon electrode and with the *in situ* interaction of OTA with dsDNA immobilized on a glassy carbon electrode surface.

2. Experimental

2.1. Materials and reagents

Ochratoxin A (OTA), calf thymus dsDNA, polyguanilic acid (poly[G]) and polyadenilic acid (poly[A]) were obtained from Sigma and used without further purification. A stock solution of 2.5 mM OTA was prepared in ethanol and stored at 5 °C. Solutions of different concentrations of OTA were prepared by dilution of the appropriate quantity in supporting electrolyte. Stock solutions of 300 $\mu g\,mL^{-1}$ dsDNA, poly[G] and poly [A] were prepared in deionized water and diluted to the desired concentration in pH 4.5 0.1 M acetate buffer.

All supporting electrolyte solutions, Table 1, were prepared using analytical grade reagents and purified water from a Millipore Milli-Q system (conductivity $\leq 0.1\,\mu S\,cm^{-1}$).

Microvolumes were measured using EP-10 and EP-100 Plus Motorized Microliter Pippettes (Rainin Instrument Co. Inc., Woburn, USA). The pH measurements were carried out with a Crison micropH 2001 pH-meter with an Ingold combined glass electrode. All experiments were done at room temperature (25 ± 1 °C).

Table 1
Supporting electrolytes (diluted to 100 mL)

pH	Composition
2.1	0.2 M HCl (42.5 mL) + 0.2 M KCl (25 mL)
3.2	0.2 M HAcO (46.3 mL) + 0.2 M NaOAc (3.7 mL)
4	0.2 M HAcO (36.8 mL) + 0.2 M NaOAc (13.2 mL)
4.5	1 M HAcO (12.5 mL) + 1 M NaOAc (7.2 mL)
5.1	0.2 M HAcO (8.8 mL) + 0.2 M NaOAc (41.2 mL)
6	0.2 M NaH_2PO_4 (43.85 mL) + 0.2 M Na_2HPO_4 (6.15 mL)
7	0.2 M NaH_2PO_4 (19.5 mL) + 0.2 M Na_2HPO_4 (30.5 mL)
8	0.2 M NaH_2PO_4 (2.65 mL) + 0.2 M Na_2HPO_4 (47.35mL)
9.1	0,1 M NaOH (3 mL) + 0.025 M $Na_2B_4O_7$ (50 mL)
12.1	0.2 M NaOH (6 mL) + 0.2 M KCl (25 mL)

2.2. Voltammetric parameters and electrochemical cells

Voltammetric experiments were carried out using a μAutolab running with GPES 4.9 software, Eco-Chemie, Utrecht, The Netherlands. The experimental conditions for differential pulse voltammetry (DPV) were: pulse amplitude 50 mV, pulse width 70 ms, scan rate 5 mV s^{-1}. Measurements were carried out using a glassy carbon electrode (GCE) (d = 1.5 mm), with a Pt wire counter electrode, and a Ag/AgCl (3 M KCl) electrode as reference, in a 0.5 mL one-compartment electrochemical cell.

The GCE was polished using diamond spray (particle size 1 μm) before every electrochemical assay. After polishing, the electrode was rinsed thoroughly with Milli-Q water for 30 s; then it was sonicated for 1 min in an ultrasound bath and again rinsed with water. After this mechanical treatment, the GCE was placed in buffer electrolyte and various DP voltammograms were recorded until a steady state baseline voltammogram was obtained. This procedure ensured very reproducible experimental results.

2.3. Acquisition and presentation of voltammetric data

All the voltammograms presented were background-subtracted and baseline-corrected using the moving average application with a step window of 5mV included in GPES version 4.9 software. This mathematical treatment improves the visualization and identification of peaks over the baseline without introducing any artefact, although the peak intensity is in some cases reduced (<10%) relative to that of the untreated curve. Nevertheless, this mathematical treatment of the original voltammograms was used in the presentation of all experimental voltammograms for a better and clearer identification of the peaks. The values for peak current presented in all plots were determined from the original untreated voltammograms after subtraction of the base line.

2.4. DNA-biosensor preparation and incubation procedure

The dsDNA-biosensor was prepared by electrostatic immobilization of dsDNA at a GCE (d = 1.5 mm) surface from a solution of 50 μg mL^{-1} by applying a potential of +0.30 V versus Ag/AgCl during 5 min.

Incubation with OTA was always carried out by holding the biosensor during 5 mins in a solution containing 100 μM OTA solution in pH 4.5 0.1 M acetate buffer. During this period of time the solution was continuously stirred.

3. Results and discussion

3.1. Cyclic voltammetry

The oxidation behaviour of OTA was first studied by cyclic voltammetry (CV) at 200 mV s^{-1} in electrolytes with different pH, all containing 500 μM OTA, Fig. 1A. In alkaline media, OTA oxidation occurs in a single step, peak 1_a at $E^1_{pa} = +0.88$ V and this potential does not depend on the electrolyte pH. Lowering the solution pH, for pH < 7, on the reverse negative-going scan of the first cycle a new peak 2_c appeared and its potential depends on the solution pH. Also, it is observed that peak 2_c current increases with decreasing pH. This peak corresponds to the reduction of the OTA oxidation product formed at the GCE surface after OTA oxidation during the positive scan of the first cycle.

The oxidation of OTA in pH 7 0.2 M phosphate buffer peak 1_a occurs at $E^1_{pa} = +0.88$ V, Fig. 1B. On the reverse scan, the reduction peak 2_c appeared at $E^2_{pc} = +0.22$ V. As mentioned, this peak 2_c corresponds to the reduction of the OTA oxidation product formed at the GCE surface. A subsequent CV scan showed a new oxidation peak 2_a occurring at E_{pa} = +0.26 V, thus confirming the reversibility of peak 2_c.

A CV in a solution of 500 μM OTA but in pH 4 0.2 M acetate buffer, Fig. 1C, shows on the first scan the anodic peak 1_a at $E^1_{pa} = +1.09$ V. On the reverse scan of the first cycle peak 2_c occurs at $E^2_{pc} = +0.34$ V. However, on a second scan, peak 2_a occurs at higher potential than expected, $E^2_{pa} = +0.67$ V, and does not form a reversible couple with peak 2_c as in the case of pH 7 0.2 M phosphate buffer. A similar behavior has been already observed during CV studies on the electrochemical oxidation of OTA and 4-chlorophenol in acetonitrile [24].

The above result can be explained taking into account the adsorption of both OTA and OTA oxidation products at the GCE surface and which leads to the blocking of the electrode surface. This was confirmed by carrying out a similar experiment in the same conditions but in a less concentrated solution (50 μM OTA), see Fig. 1D, which shows peak 2_a occurring at $E^2_{pa} = +0.46$ V in the second scan, forming a reversible couple with peak 2_c. Moreover, in this case, a new peak 3_a appeared at $E^3_{pa} = +0.98$ V.

The pair of peaks 2_c–2_a can be due to the formation of a quinone derivative that is reversibly reduced to form a hydroquinone, a species already mentioned in the literature as an OTA oxidation product by a Fe-porphyrin system [12,24]. The hydroquinone specie can also undergo oxidation to catechol which is reversibly oxidized [12]. However, considering the formation of catechol at the GCE surface, peak 3_a in Fig. 1D, the amount of the compound formed at the electrode surface is very low, and the oxidation is irreversible since no peak was observed in the reverse scan [12,24]. There was no increase of the peak 3_a current in a third scan.

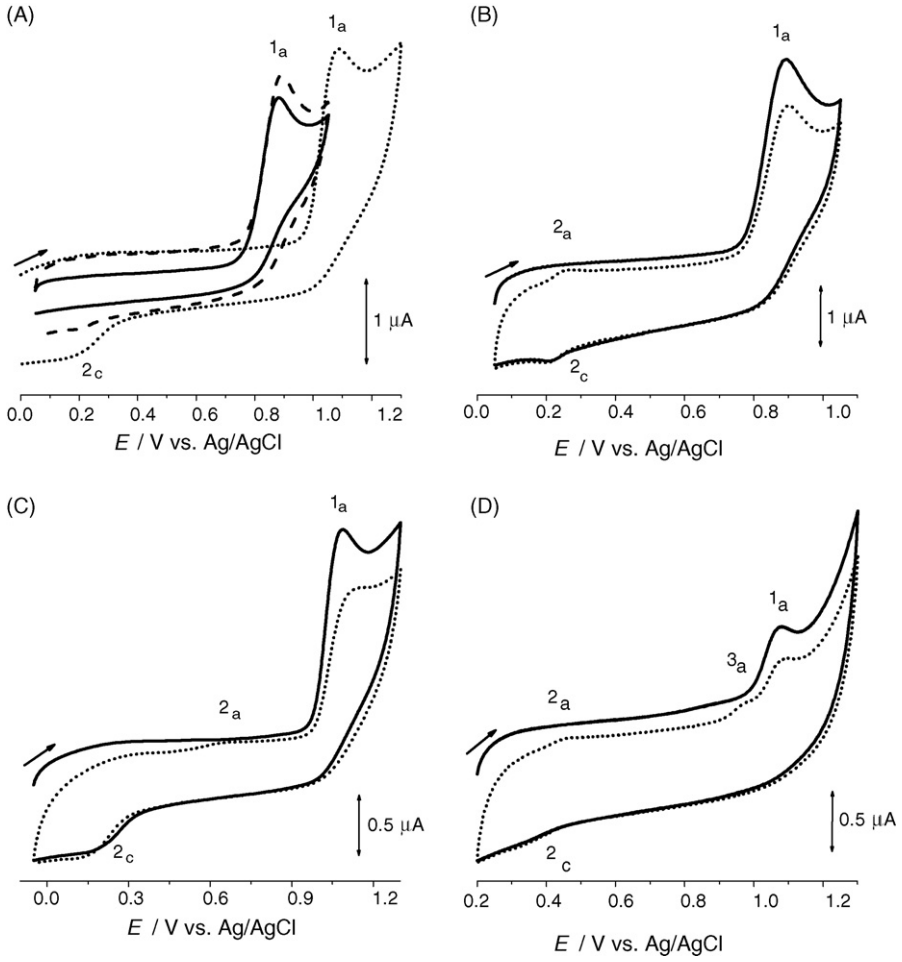

Fig. 1. CVs obtained with a GCE in solutions of 500 µM OTA: (A) (▬) pH 9.3 0.2 M borate buffer, (▪▪▪) pH 7 0.2 M phosphate buffer and (●●●●) pH 4 0.1 M acetate buffer; (B) pH 7 0.2 M phosphate buffer (▬) first and (●●●●) second scan; (C) pH 4 0.2 M acetate buffer (▬) first and (●●●●) second scan and (D) 50 µM OTA in pH 4 0.2 M acetate buffer; (▬) first and (●●●●) second scan, $\nu = 200\,\text{mV s}^{-1}$.

Since the adsorption of OTA and/or its oxidation product is very strong in acid electrolytes, further studies were carried out in pH 7 0.2 M phosphate buffer. CVs were obtained for different scan rates in a solution of 100 µM OTA. It was observed that, on increasing ν, peak 1_a potential is slightly displaced to more positive values. The difference between peak potential E_{pa} and the potential at half height of peak $E_{p/2a}$ was ~43.3 mV. Since for a diffusion-controlled irreversible system $|E_{pa} - E_{p/2a}| = 47.7/(\alpha_c n')$, where α_c is the charge transfer coefficient and n' the number of electrons in the rate-determining step [27], it can be calculated that $\alpha_c n' = 1.1$.

Also, increasing the scan rate, the current of peak 1_a increases linearly with square root of ν (not shown), consistent with the diffusion-limited oxidation of a solution species. The peak current in amperes for a diffusion-controlled irreversible system is given by $I_{pa}\,(\text{A}) = 2.99 \times 10^5 n(\alpha_c n')^{1/2} A [R]_\infty D_O^{1/2} \nu^{1/2}$ where n is the number of electrons transferred during the oxidation of OTA ($n = 1$ as shown below, Section 3.2), A is the electrode area in cm^2, D_O is the diffusion coefficient in $\text{cm}^2\,\text{s}^{-1}$, $[R]_\infty$ is the concentration in mol cm^{-3} and ν is in V s^{-1} [27]. By plotting I_{pa} versus $\nu^{1/2}$, the value of D_O is obtained. For the measured slope of $1.08 \times 10^{-6}\,\text{A}/(\text{V s}^{-1})^{1/2}$ the diffusion coefficient of OTA in pH 7 0.2 M phosphate buffer is $D_O = 3.65 \times 10^{-6}\,\text{cm}^2\,\text{s}^{-1}$. For this calculation, the GCE electroactive area was determined from a plot of I_{pc} versus $\nu^{1/2}$ using a solution of 0.5 mM hexacyanoferrate and the value of the diffusion coefficient of hexacyanoferrate in phosphate buffer of $D_O = 7.35 \times 10^{-6}\,\text{cm}^2\,\text{s}^{-1}$ [28]. In this way, an electroactive area of 0.031 cm^2 was determined.

3.2. The influence of pH

The electrochemical oxidation of OTA was studied over a wide pH range between 2 and 12 using DPV. The DP voltammograms, Fig. 2A, were all recorded in solutions of 50 µM OTA in different electrolytes with 0.2 M ionic strength.

For a solution with pH between 2 and 7, the potential of peak 1_a is displaced to lower values with increasing pH, following the relationship $E_{pa}\,(\text{V}) = 1.126\text{–}0.063\,\text{pH}$, Fig. 2A. The slope of the line, 63 mV per pH unit, shows that the oxidation mechanism of OTA involves the same number of electrons and protons. In addition, in all electrolytes, the width at half height of the OTA oxidation peak 1_a was $W_{1/2} = 88$ mV, which suggests that the oxidation of OTA occurs with the transfer of one electron, hence also one proton. The apparent one electron and one proton

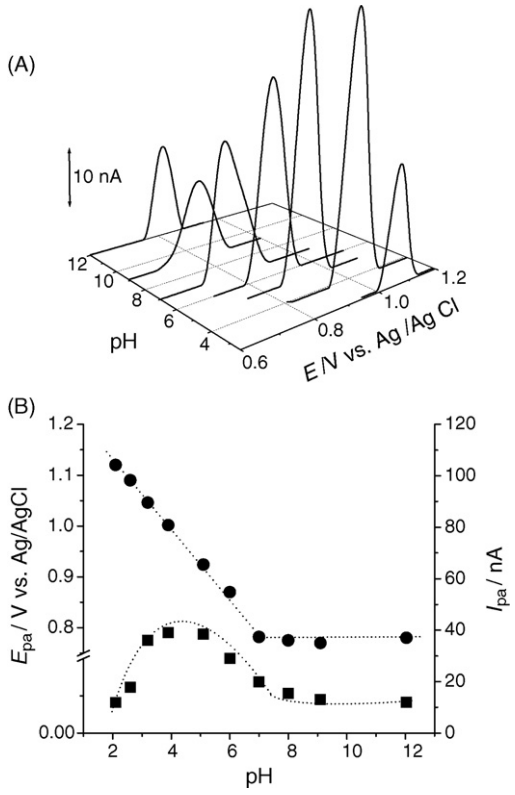

Fig. 2. (A) 3D plot of first DP voltammograms obtained in 5 μM OTA as a function of pH. (B) Plot of (●) E_{pa} and (■) I_{pa} of peak 1_a vs. pH.

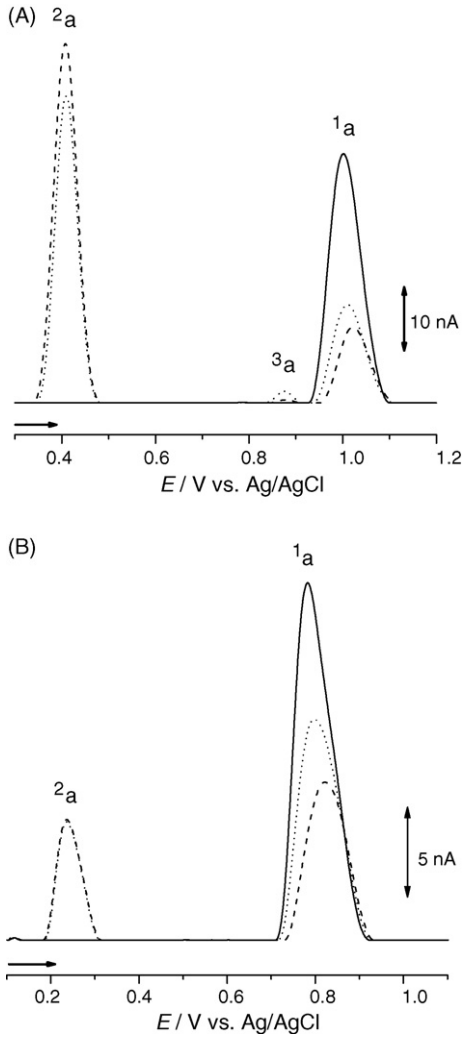

Fig. 3. Base line corrected DPV recorded in 5 μM OTA in: (A) pH 4 0.2 M acetate buffer and (B) pH 7 0.2 M phosphate buffer; (▬) first and (●●●●) second and (■■■) third scan; Pulse amplitude 50 mV, pulse width 70 ms and scan rate $\nu = 5\,\mathrm{mV\,s^{-1}}$.

reaction must be of a more complex nature if the formation of the quinone derivative at the GCE surface as electrochemical oxidation product of OTA is considered. The formation of the quinone derivative is a complex process that besides electron transfer also involves the nucleophilic attachment of water and the release of a chloride ion [12,24].

For pH >7, the OTA oxidation peak does not depend on pH indicating a mechanism involving only one electron, possible if the OTA oxidation product undergoes chemical deprotonation in alkaline electrolytes. Thus the value of $pK_a = 7$ of OTA can be determined, in agreement with the previously reported results [24] and with the fact that the phenolic group is deprotonated at physiological pH.

The graph of the variation of peak 1_a current versus pH, Fig. 2B, shows that the current increases with pH with a maximum in the pH range 4–5.

Successive DP voltammograms were recorded in a solution of 5 μM OTA in pH 4 0.2 M acetate buffer, Fig. 3A. The oxidation of OTA, peak 1_a, occurs at $E^1_{pa} = +1.10$ V. In a second DP scan, two new peaks 2_a and 3_a occur at $E^2_{pa} = +0.41$ and at $E^3_{pa} = +0.87$ V. These peaks correspond to the oxidation of OTA oxidation products. The peak 1_a current decreases with the number of scans due to the decrease of the available electrode surface area owing to adsorption of OTA oxidation products. The adsorption of OTA oxidation products at the GCE surface was confirmed when, at the end of several DP scans recorded in the solution of OTA, the electrode was washed with a jet of deionized water and then transferred to the supporting electrolyte. The DP voltammogram obtained in these conditions (not shown) shows only peaks 2_a and 3_a. Moreover, consecutively recorded DP voltammograms in buffer showed only a continuous, but slow decrease of peak 2_a oxidation current due to product consumption, whereas peak 3_a disappears after the first scan in buffer.

Successive DP voltammograms were also recorded in a solution of 5 μM OTA in pH 7 0.2 M phosphate buffer, Fig. 3B. The oxidation of OTA, peak 1_a, occurs at $E^1_{pa} = +0.80$ V. On a second DP scan, a new peak 2_a appears at $E^2_{pa} = +0.24$ V, and its amplitude remains constant during further scans, although the amplitude of peak 1_a decreases gradually with the number of potential scans due to the adsorption of OTA oxidation product at the GCE surface. Nevertheless, in alkaline electrolyte the adsorption of OTA oxidation product is not as strong as in acid media. This was observed when, after recording three consecutive scans in the OTA solution, the electrode was washed with a jet of deionized water and then transferred to the

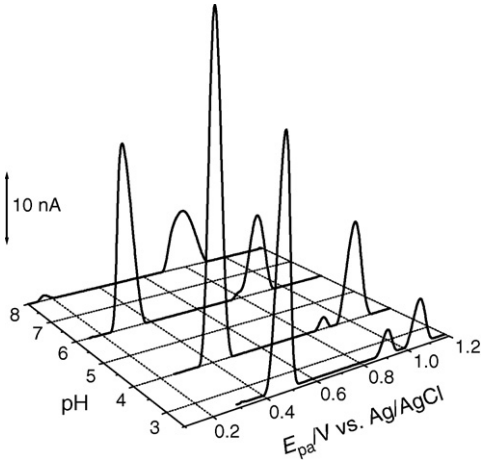

Fig. 4. 3D plot of second DP voltammograms obtained in 5 μM OTA as a function of pH.

supporting electrolyte. No oxidation peak 2_a was observed in the DPV scan obtained in these conditions (not shown).

Consecutive DP voltammograms recorded in the same solution of OTA showed new peaks corresponding to OTA oxidation products adsorbed at the GCE surface, and the electrochemical oxidation of these compounds was also studied for different pH values. Thus, two consecutive DP voltammograms were recorded in solutions of 5 μM OTA in different electrolytes and the second DP voltammograms were plotted vs. pH, Fig. 4.

It was observed that peak 2_a occurs only for electrolytes with pH < 8. The potential of peak 2_a is displaced to more negative values with increasing pH, following a linear relationship with slope 57 mV per pH unit. This means that the oxidation of the OTA oxidation product involves the same number of electrons and protons. Nevertheless, in all electrolytes, the width at half height of peak 2_a was $W_{1/2} = 50$ mV, which suggests that the oxidation of OTA oxidation product occurs with the transfer of two electrons, hence also two protons.

Also, from Fig. 4 it is observed that peak 3_a appeared for electrolytes with pH < 6, for higher pH the peak tends to merge with OTA oxidation peak 1_a. However, the dependence of the peak potential on pH is also linear and corresponds to 38 mV per pH unit, showing that it is likely that the reaction mechanism involves an electron transfer followed by a chemical reaction, probably dimerization [29].

3.3. Square wave voltammetry

The advantages of square wave voltammetry (SWV) are greater speed of analysis, lower consumption of the electroactive species in relation with DPV, and reduced problems with poisoning of the electrode surface [30]. SWV showed similar features to DPV and CV, i.e., oxidation peaks 1_a, 2_a and 3_a and a large amount of adsorption on the second scans. The first SW scan obtained in a solution of 10 μM OTA in pH 4 0.2 M acetate buffer, shows OTA oxidation peak 1_a, $E^1_{pa} = +1.05$ V, Fig. 5A. On a second SW scan, peak 2_a occurs at $E^2_{pa} = +0.45$ V and its amplitude increases with the number of potential scans and peak 3_a can be observed at $E^3_{pa} = +0.92$ V.

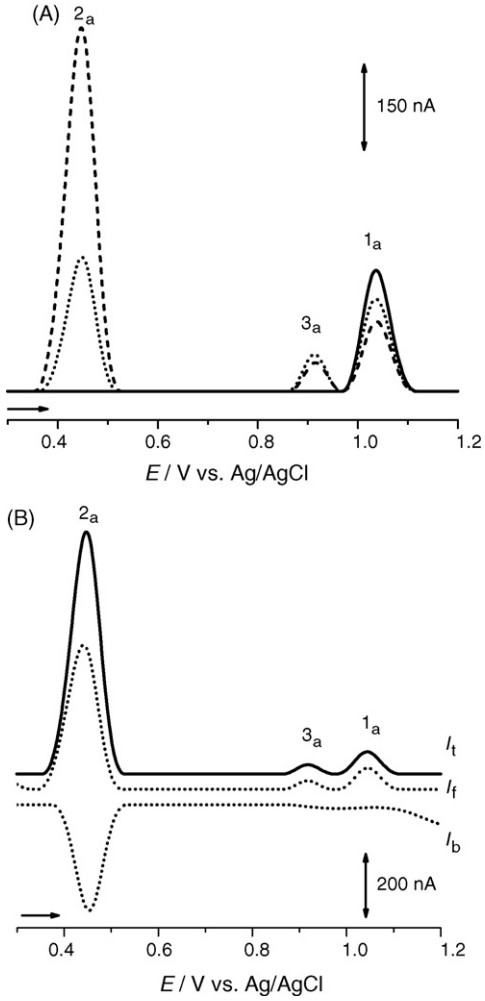

Fig. 5. Base line corrected SWV recorded in 10 μM OTA in pH 4 0.2 M acetate buffer: (A) (▬) first and (●●●●) second and (▪▪▪) third scan and (B) fifth scan; I_t: total; I_f: forward and I_b: backward currents; pulse amplitude 50 mV, step potential 2 mV, frequency 50 Hz, $\nu_{effective} = 100$ mV s^{-1}.

On the other hand, the reversibility of peak 2_a is confirmed by plotting the forward and backward components of the total current where the oxidation and the reduction currents are equal, Fig. 5B. Moreover, the identical value of the potential of peak 2_a on the forward and backward current components is an indication of the adsorption of OTA oxidation products on the GCE surface.

A greater advantage of square wave voltammetry is the possibility to see during only one scan if the electron transfer reaction is reversible or not. Since the current is sampled in both positive and negative-going pulses, peaks corresponding to the oxidation and reduction of the electroactive species at the electrode surface can be obtained in the same experiment. Also, SWV experiments show a higher sensitivity than DPV since much faster scan rates can be used (100 mV s^{-1} for SWV compared to 5 mV s^{-1} for DPV). Taking into account these facts, the analytical determination of OTA was carried out using SWV and measuring the oxidation peak of its oxidation product, since this product can undergo reversible oxidation.

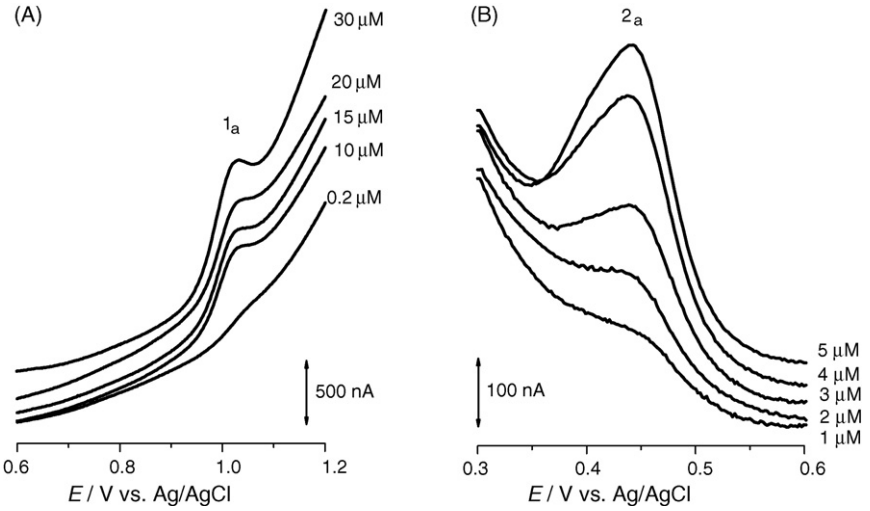

Fig. 6. SW voltammograms recorded in different concentrations of OTA using (A) *Procedure 1* and (B) *Procedure 2*; pulse amplitude 50 mV, step potential 2 mV, frequency 50 Hz, $\nu_{effective} = 100\,mV\,s^{-1}$.

3.4. Analytical determination of OTA

Two different procedures for the electroanalytical determination of OTA were evaluated. Supporting electrolyte, pH 4.0, 0.2 M acetate buffer, was preferred since higher oxidation peaks are obtained, as shown in Figs. 2A and 4.

3.4.1. Procedure 1

SW voltammograms were recorded for standard additions of OTA corresponding to bulk concentrations between 2 and 75 μM, Fig. 6A. OTA oxidation peak 1_a current was used as the analytical signal. Between measurements the GCE surface was always polished in order to ensure a clean electrode surface and to avoid the adsorption of OTA oxidation products.

3.4.2. Procedure 2

The freshly polished GCE was held at a potential of +1.15 V during 30 s in solutions of OTA corresponding to bulk concentrations between 0.2 and 30 μM. Two consecutive SW voltammograms were recorded in the OTA solution for standard additions of OTA corresponding to bulk concentrations between 0.2 and 30 μM, Fig. 6B. During the conditioning period, the OTA molecules that diffuse from the solution towards the electrode surface are oxidized leading to the formation of the OTA oxidation product at the GCE surface. Peak 2_a from a second SW voltammogram obtained in the OTA solution was used as the analytical signal. Also, between measurements the GCE surface was always polished in order to ensure a clean electrode surface and to avoid the adsorption of OTA oxidation products.

The detection limit (LOD) was determined as the OTA concentration that caused a peak with a height three times the baseline noise level, i.e. $LOD = 3 \times S.D. \times (sensitivity)^{-1}$. The quantification limit (LOQ) is the lowest concentration of a substance that can be quantified with acceptable precision and accuracy. A typical signal/noise ratio of 10 is generally considered to be acceptable; therefore: $LOQ = 10 \times S.D. \times (sensitivity)^{-1}$.

The data obtained from the calibration curves are presented in Table 2. *Procedure 1* leads to a wider linear range but a much higher LOD when compared with the results obtained using *Procedure 2*. This can be explained by taking into consideration that OTA oxidation peak 1_a occurs at high potentials, the decomposition of the solvent influencing the current measurement. On the contrary, the OTA oxidation product adsorbs at the electrode surface and there is no contribution of diffusing species to the electrochemical reaction.

The reproducibility of these methods was evaluated by plotting different calibration curves. The relative standard deviations (R.S.D.), Table 2, calculated from the sensitivities of three calibration curves were around 13 and 6% for *Procedure 1* and *Procedure 2*, respectively. It must be mentioned that each measurement was done using a freshly polished GCE, a process that give rise to small modifications of the electrode surface area which can in turn cause variations in the oxidation currents, and this should be the main source of error in the procedures

Table 2
Sensitivity, intercept, limit of detection, limit of quantification and other linear fit parameters calculate from OTA calibration curves obtained with two different procedures

Method	Sensitivity (nA μM^{-1})	Intercept (nA)	LOD (μM)	LOQ (μM)	R^2	S.D.	Linearity range (μM)	R.S.D.(%)
Procedure 1	14.40 ± 0.35	15.49 ± 3.89	1.2	3.82	0.997	5.497	30	13
Procedure 2	50.09 ± 0.59	20.18 ± 2.99	0.26	1.00	0.999	5.034	10	6

For more details see Section 3.4.

Table 3
Interference of catechol, phenol and resveratrol, on the peak current of OTA at the GCE

Interfering compound	C_{OTA}:$C_{interferent}$	Relative response (%)	
		Procedure 1 (peak 1_a)	*Procedure 2* (peak 2_a)
Cathecol	1:1	101	50
	1:3	97	43
Phenol	1:1	96	65
	1:3	93	60
Resveratrol	1:1	99	77
	1:3	97	65

For more details see Section 3.4.

described. The difference between the R.S.D. obtained with the two procedures can be explained by taking into account that the potential of +1.15 V applied during 30 s in *procedure 2*, leads to a more reproducible base line.

The electroanalytical determination of OTA carried out by square wave voltammetry measuring the oxidation peak current of OTA gave a LOD of 1.2 μM, whereas measuring the anodic peak current corresponding to oxidation of the oxidation product of OTA adsorbed on the GCE surface gave a LOD of 0.26 μM. However, LOD of the electrochemical method, in the range of 10^{-4} g L^{-1}, is much higher than what is expected in a real sample where the concentration of OTA is very low probably in the range of 10^{-9} g L^{-1}.

A study of interferences of OTA with compounds usually found in juice or wine, e.g. anthocyanins, flavones, flavonoids, was also undertaken. Most of these compounds present catechol and phenol in their structures as electroactive groups. Another possible specific interacting compound with the determination of OTA is resveratrol [31].

Experiments in solutions containing catechol, phenol and resveratrol were performed. Both experimental procedures described for the determination of OTA were used and compared. The concentration of OTA was always 2 μM whereas the concentration of the interfering compound was either 2 or 6 μM, so the relative concentrations of OTA:interferent was 1:1 or 1:3. The data obtained are presented in Table 3. The relative response (%) for C_{OTA}: $C_{interferent}$ for peak 1_a currents using *procedure 1* and peak 2_a currents using *procedure 2* were calculated as the average of 3 consecutive measurements then compared with values calculated with the equations specific for each procedure mentioned in Table 2.

Since OTA oxidation, peak 1_a, occurs at higher potentials than catechol, phenol or resveratrol, all these compounds were oxidised and interfere to a small extent when *procedure 1* is used. However, the relative response shows fluctuations of OTA oxidation peak 1_a smaller than the R.S.D. of the method, Table 2.

On the other hand, using *procedure 2*, a very strong interference of all compounds with the OTA determination was found. Since at the conditioning potential of +1.05 V, catechol, phenol and also resveratrol are all oxidized, their oxidation products also adsorb onto the GCE surface leading to its blockage.

3.5. In situ evaluation of OTA interaction with DNA

As already mentioned, OTA is considered a genotoxic compound since it promotes oxidative stress [7,8], oxidative base damage [8] and single strand DNA cleavage. Although the production of ROS appeared to be the main mechanism of OTA-induced tumor formation in animals, conflicting results have been reported regarding the potential of OTA to bind to DNA [19,25].

An electrochemical dsDNA biosensor was used to evaluate the possible interaction between OTA and DNA. The dsDNA biosensor consists of an electrode with DNA immobilized on the surface. The double stranded DNA structure makes access of the bases to the electrode surface difficult, hindering their oxidation. The interactions of the surface-immobilized dsDNA with the damaging agent causes the double helix to unwind, so that closer access of the bases to the surface is possible, leading to voltammetric signals. However, if the damaging agent is electroactive its oxidation can also occur. This redox reaction allow the *in situ* formation of reactive intermediates, such as free radicals, and their action on DNA is detected.

The thin-layer dsDNA biosensor prepared by electrostatic immobilization of dsDNA at a GCE surface was characterised by DP voltammetry. A DP voltammogram obtained with the dsDNA biosensor in pH 4.5 0.1 M acetate buffer, showed two small oxidation peaks due to the oxidation of desoxyguanosine (dGuo) at E_{pa} = +1.03 V, and desoxyadenosine (dAdo) at E_{pa} = +1.28 V, Fig. 7.

MAC Mode AFM images have shown that the thin-layer dsDNA biosensor presents large pores in the DNA film leaving parts of the electrode uncovered where non-specific adsorption of the analyte could occur [26]. In the case of OTA, non-specific adsorption does not occur since this compound does not adsorb at the GCE surface, as already shown in Section 3.2. However, this was confirmed again when after 5 min of free adsorption in a solution of 100 μM OTA, the GCE was transferred to pH 4.5

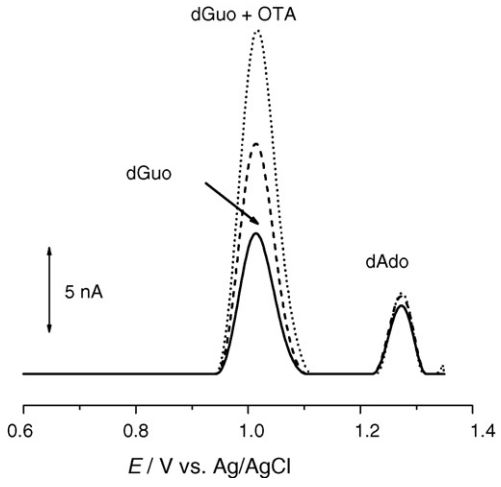

Fig. 7. DP voltammograms obtained in pH 4.5 0.1 M acetate buffer with dsDNA biosensors (▬) before and after incubation during (▬ ▬) 5 and (●●●●) 10 min in a solution of 100 μM OTA. Pulse amplitude 50 mV, pulse width 70 ms and scan rate ν = 5 mV s^{-1}.

0.1 M acetate buffer and no OTA oxidation peak 1_a was observed on the DP voltammogram (not shown).

In another experiment, a new biosensor was incubated for 5 min in a 100 μM OTA solution in pH 4.5 0.1 M acetate buffer. Then, the electrode was washed with deionized water in order to remove the unbound molecules and transferred to acetate buffer where DPV was performed. The voltammogram obtained showed an increase of the peak at $E_{pa} = +1.03$ V, Fig. 7. Also, for longer incubation times (10 min) a higher peak at $E_{pa} = +1.03$ V was observed. On the other hand, in all cases dAdo peak maintained practically the same current, Fig. 7.

The peak at $E_{pa} = +1.03$ V is due to two contributions; the oxidation of dGuo residues in the immobilized DNA strands, and the oxidation of OTA molecules that interacted with DNA. Since non-specific adsorption of OTA at the uncovered regions of the DNA biosensor does not occur, the increase of the peak at $E_{pa} = +1.03$ V is only due to the oxidation OTA molecules bound to the DNA strands. These experiments have clearly demonstrated that OTA interacts and binds to dsDNA strands but no evidence of DNA damage caused OTA was obtained.

Experiments concerning OTA interaction with DNA were also carried out using poly[G]- and poly[A]-modified GCE. The modification of the GCE surface was carried out as described in Section 2.4. Similar results were obtained, confirming that the electrochemical dsDNA biosensor does not appear to be suitable to study the interaction of electrochemically-produced OTA metabolites with DNA. Since the oxidation of OTA occurs at a potential similar to that of guanine residues in DNA, the application of a conditioning potential that allow the oxidation of OTA molecules bounded to the immobilized DNA would involve also the electrochemical oxidation of guanine to 8-oxoguanine [26]. In the case that OTA oxidation product would damage DNA leading to the formation of 8-oxoguanine as already reported [8], its detection will be influenced by the presence of 8-oxoguanine electrochemically generated at the biosensor surface through the oxidation of guanine [26].

4. Conclusions

This study shows that ochratoxin A, a fungal metabolite that presents carcinogenic, teratogenic and nephrotoxic properties undergoes oxidation at a glassy carbon electrode.

The oxidation of OTA is an irreversible process that occurs with the formation of a quinone that, in acid media, adsorbs strongly on the GCE surface and undergoes reversible oxidation. The diffusion coefficient of OTA was calculated in pH 7 phosphate buffer to be $D_O = 3.65 \times 10^{-6}\ cm^2\ s^{-1}$. The oxidation of OTA is also pH dependent for electrolytes with pH < 7, and occurs with the transfer of one electron and one proton. In alkaline solution OTA undergoes chemical deprotonation, the oxidation becoming pH independent and involving only the transfer of one electron. Two methods for the electroanalytical determination of OTA were also developed; the LODs were 1.2 and 0.26 μM, respectively.

An electrochemical dsDNA biosensor was used to evaluate the possible interaction between OTA and DNA. The experiments have clearly shown that OTA interacts and binds to dsDNA strands but no evidence of DNA damage caused OTA was obtained.

Acknowledgements

Financial support from Fundação para a Ciência e Tecnologia (FCT), BIID Grant POCTI/QUI/47201/2002 (S.C.B. Oliveira), Post-Doctoral Grant SFRH/BPD/18824/2004 (V.C. Diculescu.), POCI (cofinanced by the European Community Fund FEDER), ICEMS (Research Unit 103), and European Project HPRN-CT-2002-00186 is gratefully acknowledged.

References

[1] P.S. Steyn, Toxicol. Lett. 82 (1995) 843.
[2] K.J. van der Merwe, P.S. Steyn, L. Fourie, D.B. Scoot, J.J. Theron, Nature 205 (1965) 112.
[3] A.E. Pohland, P.L. Schuller, P.S. Steyn, H.P. Van Egmond, Pure Appl. Chem. 54 (1982) 2219.
[4] P. Bayman, J.L. Baker, Mycopathologia 162 (2006) 215.
[5] R.R. Marquardt, A.A. Frohlich, J. Anim. Sci. 70 (1992) 253.
[6] D. Ringot, A. Chango, Y.-J. Schneider, Y. Larondelle, Chem. Biol. Interact. 159 (2006) 18.
[7] J.-C. Gautier, D. Holzhaeuser, J. Markovic, E. Gremaud, B. Schilter, R.J. Turesky, Free Rad. Biol. Med. 30 (2001) 1089.
[8] G.J. Schaaf, S.M. Nijmeijer, R.F.M. Maas, P. Roestenberg, E.M. de Groene, J. Fink-Gremmels, Biochim. Biophys. Acta 1588 (2002) 149.
[9] E.E. Creppy, A. Kane, G. Dirheimer, C. Lafarge-Frayssinet, S. Mousset, C. Frayssinet, Toxicol. Lett. 28 (1985) 29.
[10] S. Lebrun, W. Follmann, Arch. Toxicol. 75 (2002) 734.
[11] A. Mally, H. Zepnik, P. Waken, E. Eder, K. Dingley, H. Ihmels, W. Volkel, W. Dekat, Chem. Res. Toxicol. 17 (2004) 234.
[12] I.G. Gillman, T.N. Clark, R.A. Manderville, Chem. Res. Toxicol. 12 (1999) 1066.
[13] R.A. Manderville, M.W. Calcutt, J. Dai, G. Park, I.G. Gillman, R.E. Noftle, A.K. Mohammed, M. Dizdaroglu, H. Rodriguez, S.A. Akman, J. Inorg. Biochem. 95 (2003) 87.
[14] F. Galvano, A. Piva, A. Ritieni, G.J. Galvano, Food Prot. 64 (2001) 120.
[15] F. Galvano, L. La Fauci, G. Lazzarino, V. Fogliano, A. Ritieni, S. Ciappellano, N.C. Battistini, B. Tavazzi, G. Galvano, J. Nutr. Biochem. 15 (2004) 2.
[16] M.Z. Zheng, J.L. Richard, J. Binder, Mycopathologia 161 (2006) 261.
[17] H. Valenta, J. Chromatogr. A 815 (1998) 75.
[18] E.G. Peñas, C. Leache, A.L. de Cerain, E. Lizarraga, Food Chem. 97 (2006) 349.
[19] S. Obrecht-Pflumio, G. Dirheimer, Chem.Biol. Interact 127 (2000) 29.
[20] A. Visconti, M. Pascale, G. Centonze, J. Chromatogr. A 888 (2000) 321.
[21] S.H. Alarcon, G. Palleschi, D. Compagnone, M. Pascale, A. Visconti, I. Barna-Vetro, Talanta 69 (2006) 1031.
[22] V.C. Diculescu, S. Kumbath, A.M. Oliveira-Brett, Anal. Chim. Acta 575 (2006) 190.
[23] A.M. Oliveira-Brett, J.A.P. Piedade, L.A. da Silva, V.C. Diculescu, Anal. Biochem. 332 (2004) 321.
[24] M.W. Calcutt, I.G. Gillman, R.E. Noftle, R.A. Manderville, Chem. Res. Toxicol. 14 (2001) 1266.
[25] D. Ringot, A. Chango, Y.-J. Schnaider, Y. Larondelle, Chem. Biol. Interact. 159 (2006) 18.
[26] V.C. Diculescu, A.M. Chiorcea-Paquim, A.M. Oliveira-Brett, Sensors 5 (2005) 377.
[27] C.M.A. Brett, A.M. Oliveira-Brett, Electrochemistry: Principles, Methods and Applications, Oxford University Press, UK, 1993.
[28] http://www.hbcpnetbase.com/, Handbook of chemistry and physics.
[29] E.M. Garrido, J.L. Costa Lima, A.M. Oliveira-Brett, Talanta 46 (1998) 1131.
[30] J. Osteryoung, R. Osteryoung, Anal. Chem. 57 (1985) 101A.
[31] O. Corduneanu, P. Janeiro, A.M. Oliveira-Brett, Electroanal. 18 (2006) 757.